Ultrasonic Synthesis, Characterization and Application of Al$_2$O$_3$-TiO$_2$ Nanocomposite Particles

ASHRAFUL Islam, SONY Ahmed[*], YEASMIN Akter, MOHAMMAAD A Hossain, SHAFIUL Islam, SAIFUL Islam, MILON Bhoumik

Department of Applied Chemistry and Chemical Engineering, Noakhali Science and Technology University, Sonapur, Noakhali, Bangladesh-3814
*sonyahmed91@gmail.com

Abstract A novel and rapid ultrasonication method was used to prepare Al$_2$O$_3$-TiO$_2$ nanocomposite particles. Al$_2$O$_3$nanoparticles were dispersed in ethanol and ammonia under magnetic stirring followed by the addition of titanium tetra-n- butoxide as titania precursor. The final mixture was sonicated for 2 hrs for the preparation of Al$_2$O$_3$-TiO$_2$nanocomposite particles. The prepared nanocomposite particles were characterized by Fourier transform infrared spectroscopy (FT-IR), Scanning electron microscopy (SEM) and X-ray diffraction (XRD). Before taking XRD data, the pure and nanocomposites were annealed at 500 ºC and 700ºC. SEM images show that uncoated alumina and titania nanoparticles have smooth surface whereas the surface morphology had changed after titania incorporation. XRD results confirmed the successful anatase phase formation of TiO$_2$. FT-IR method revealed successful preparation of Al$_2$O$_3$-TiO$_2$ nanocomposite by ultrasonic method. The photocatalytic activities of the pure and nanocomposite particles were tested using a model dye methylene blue under ultraviolet radiation.

Keywords nanoparticles, ultrasonic, photocatalytic, irradiated, Degradation

Introduction

Nanotechnology ("nanotech") is manipulation of matter on an atomic, molecular, and supramolecular scale. According to the National Nanotechnology Initiative, Nanotechnology is the understanding and control of matter at dimensions between approximately 1 and 100 nanometers, where unique phenomena enable novel applications. Encompassing nanoscale science, engineering, and technology, nanotechnology involves imaging, measuring, modeling, and manipulating matter at this length scale. Over a decade later the Japanese scientist called Norio Taniguchi of the Tokyo University ofScience first used the term "Nano-technology" in a 1974 conference [1] to describe semiconductor processes such as thin film deposition and ion beam milling exhibiting characteristic control on the order of a nano meter. His definition was,"' Nano-technology mainly consists of the processing, separation, consolidation, and deformation of materials by one atom or one molecule. The practical and potential applications of pigmentary and nano-sized titanium dioxide are vast it is in wide spread use in paints, plastics, sunscreens/cosmetics, coatings, and imprinting and paper products [2]. The end use determines whether pigmentary or nanosized grade particulate titaniurn dioxide is utilized. For these applications a surface coating is typically applied to control the dispersion and optical properties and to minimize the inherent photoactivity. In addition, there has been considerable research into the use of titanium dioxide as a photocatalyst for environmental remediation, although currently this technique is not widely commercially viable [3], and for self-cleaning windows or buildings [4]. Global demand for titanium dioxide exceeds 4

million metric tons and is estimated to be rising at 3% per annum titanium dioxide naturally occurs in three crystalline forms: anatase, rutile and brookite [5] -of which only the former two find application and are produced commercially. Anatase and brookite transform to the rutile phase with heating as this is the most thermodynamically stable phase - the anatase to rutile transition is at approximately $700^{\circ}C$ [6]. Al_2O_3 can occurs naturally in its crystalline polymorphicphaseα-Al_2O_3 as the mineral corundum, varieties of which form the precious gemstones ruby and sapphire [7]. Al_2O_3 is significant in its use to produce aluminum metal, as an abrasive owing to its hardness, and as a refractory material owing to its high melting point. Suslick & Price (1999), prepared silica coated alumina nanoparticles using microwave irradiation. Micro wave heating resulted in a thin but homogenous cover age of silica on the Al_2O_3nanoparticles surface within a very short time [8]. Costa et al (2012), investigated the unique structure of Al_2O_3obtained from aqueous solution method. Scanning electron microscopy (SEM) and X-ray powder diffraction (XRD) analyses indicate that unique morphology and structure of the region where precipitation on the substrate may occur in parallel with other regions. This is accompanied by a decrease of the electrical resistivity in the absorbed region. A possible mechanism for the resistivity transformation was not discussed [9]. Mason & Lorimer (2002), showed the synthesis of titanium nanoparticles using a wet chemical approach in imidazolium based ionic liquids (ILs) under reducing conditions. Transmission electron microscopy finds nanoparticles in all cases. IR spectroscopy shows that even after extensive washing and drying, some IL remains adsorbed on the nanoparticles. Raman spectroscopy suggests the formation of anatase nanoparticles, but X- ray diffraction reveals that, possibly, amorphous Titania forms or that the Nano particles are so small that a clear structure assignment is not possible [10]. Nicolais & Carotenuto (2005), prepared the photocatalytic coatings via incorporating the modified Titania nano particles in to epoxy-based inorganic-organic hybrid coatings. Titania nano particles were first synthesized from tetra-n-butylortho titanate using ultrasonic methods by two different calcination treatments, [11]. Curridal et al (2003) studied the kinetics and mechanism of methylene blue adsorption from aqueous solution by nitric acid created water-hyacinth. The experiments were conducted to evaluate the adsorption characteristics of acataionic dye (methylene blue-MB) on to nitric acid created water- hyacinth (N-WH). Results showed that N-WH can remove MB effectively from aqueous solution [12]. The adsorption kinetics at room temperature could be expressed by the pseudo second order model. Shipra & Tripathi (2011), structural and nanocomposites feature of TiO_2- Al_2O_3 powder prepared by sol gel method. Titania nanoparticles were first synthesized from tetra-n-butyl ortho titanite using ultrasonic methods by two different calcination treatments at 500°C.and 700°C [13]. Characterization of the samples was carried by X-ray diffraction (XRD) analysis, Scanning Electron Microscopy (SEM), FT-IR analysis. Radzimska & Jesionowski (2014), produced Nanometric zinc oxide coated with Al_2O_3, with diameter 50–80 nm by calcination of basic zinc carbonate (BZC)with simultaneous modification with a precipitate of Al $(OH)_3$ at 400–600°C [14]. The coating obtained was highly uniform and had a thickness of 5 nm. The pH at the isoelectric point for TiO_2nanoparticles with an Al_2O_3 layer moved from around 10 to a value of 6, which may improve the dispersion of TiO_2 particles. Al_2O_3 nanoparticles was then studied by mixing it with engine base fluid as nanofluid [15]. The usage of nano fluid was expected to be heat absorber and would increase cooling process in cooling machine. The results showed that cooling time increases when the concentration of nano fluid was increased. Finally, it is concluded that thermal property of $Al_2O_3$was studied and applicable to be mixed with engine coolant of cooler machine to reduce cooling time process.

Materials & Methods

Materials used throughout this research are list in Table 1.

Table 1: List of chemicals in this research

Chemicals & materials	Molecular formula	Supplier
Titanium Butoxide	$Ti(OBu)4$ ($Bu= CH_2CH_2CH_2CH_3$)	Sigma-Aldrich
Ammonium Hydroxide	$[NH4^+]$ $[OH^-]$	Sigma-Aldrich
Ethanol	C_2H_5OH	Sigma-Aldrich
Methylene blue	$C_{16}H_{18}C_lN_3S$	Sigma-Aldrich

Synthesis of Materials

Synthesis of Titania Nano particles: 2ml of Tetrabutyl Orthotitanate (TBOT) was added to 100ml of Ethanol and 1.43ml of water and 8mL ammonia. The final mixture was ultrasonic irradiated at room temperature for 2 hours sand then centrifuged at 9000 rpm for 15min.The residue was washed with ethanol for three times and then dried at 90°C for 24 hours

Synthesis of Al_2O_3-TiO_2 Nano composites: In a typical experiment, 0.8 g of uncoated Al_2O_3 powder and 8 ml NH4OH was dispersed into 81 ml ethanol. Then 2ml of Tetrabutyl Orthotitanate (TBOT) was added to 100ml of Ethanol and 1.43ml of water and 8mL ammonia. Then two composites of final mixture were ultrasonic irradiated at room temperature for 2hour sand then centrifuged at 9000 rpm for 15 min. The residue was washed with ethanol for three times and then dried at 90°C for 24 hours

Photodegradation of Methylene blue

Methylene blue was used to assess the photocatalytic activity of the synthesized Al_2O_3-TiO_2 nanocomposites. Five bulbs (22 inch, 15 W) with the strongest band at the wavelength of 668 nm were used as the UV-irradiation source. Aqueous solution of Methylene blue ($1.00x10^{-5}$) and the photocatalytic particles (Al_2O_3-TiO_2) were placed in a pyrex beaker and the particles were kept in suspension at dark with 400 rpm magnetic stirring for 30 min to ensure adsorption/desorption equilibrium and then the mixture was UV irradiated. After given intervals of UV irradiation [16], small amount of the suspension was collected and centrifuged at 13000 rpm for 10 min to remove Al_2O_3-TiO_2 spheres and the remaining methylene blue solution was characterized with the UV-visible spectroscopy. Theintensity drops in the characteristics peak of methylene blue was used as the basis for photocatalytic efficiency of the composite particles. Concentration of the remaining methylene blue was measured at an interval of 30 minutes

Experimental data analysis

Table 2: Experimental Data for Absorbance of Methylene Blue dye solution with Al_2O_3 catalyst loading 0.05g calcinated at 500 ^{o}C

Irradiation time (minute)	Al_2O_3 Absorbance	Concentration (Molar)
30 minutes in dark	1.345	11.23
60 minutes	1.012	10.45
90 minutes	0.886	9.88
120 minutes	0.652	8.28
150 minutes	0.431	8.18
180 minutes	0.253	5.08
210 minutes	0.0932	4.18
240 minutes	0.0173	3.4

Table 3: Experimental Data for Absorbance of Methylene Blue dye solution with TiO_2- Al_2O_3 catalyst loading 0.05g calcinated at 500 ^{o}C

Irradiation time (minute)	TiO_2 Absorbance	Concentration (Molar)
30 minutes in dark	1.345	11.78
60 minutes	1.114	10.58
90 minutes	0.956	9.89
120 minutes	0.878	8.76
150 minutes	0.674	8.08
180 minutes	0.521	7.77
210 minutes	0.408	7.09
240 minutes	0.39	6.89
270 minutes	0.314	6.08
300 minutes	0.267	5.23
330 minutes	0.23	4.68
360 minutes	0.187	3.47
390 minutes	0.169	3.33
420 minutes	0.098	1.96
450 minutes	0.056	1.12
480 minutes	0.039	0.78

Table 4: Experimental Data for Absorbance of Methylene Blue dye solution with TiO_2- Al_2O_3 catalyst loading 0.05g calcinated at 500 ºC

Irradiation time (minute)	TiO_2-Al_2O_3 Absorbance	Concentration (Molar)
30 minutes in dark	1.113	9.38
60 minutes	0.896	9.23
90 minutes	0.818	9.19
120 minutes	0.798	9.09
150 minutes	0.765	9.05
180 minutes	0.757	9.01
210 minutes	0.735	8.97
240 minutes	0.726	8.93
270 minutes	0.706	8.89
300 minutes	0.699	8.88
330 minutes	0.678	8.88
360 minutes	0.646	8.78
390 minutes	0.639	8.76
420 minutes	0.619	8.71

Degradation efficiency

1. The % of degradation was calculated from the following equation-

$$\% \text{ Degradation} = (Co-C)/Co \times 100 = (Ao-A) \times 100$$

Where, Co and C are the initial and post –irradiation absorbance of Methylene blue solution at 670 nm as measured by the UV-Vis spectrophotometer, respectively [17].

2. Rate constant was calculated from data, taking the degradation reaction as a first order reaction with formula: $k=2.303/t \log (Co/C)$ Where, k= rate constant t= time, Co=initial concentration, C= final concentration. Degradation efficiency of Al_2O_3-TiO_2 catalyst calcinated at 700 ºC, 500 ºC and Al_2O_3 catalyst calcinated at 500 ºC shown in table 5

Table 5: Degradation efficiency of Al_2O_3-TiO_2 catalyst calcinated at 700 ºC, 500 ºC and Al_2O_3 catalyst calcinated at 500 ºC

Irradiation time (minute)	Degradation efficiency (%) Al_2O_3-TiO_2 calcinated at 700 ºC	Degradation efficiency (%) Al_2O_3-TiO_2 calcinated at 500 ºC	Degradation efficiency (%) Al_2O_3 calcinated at 700 ºC
30 minutes	17.9	16.8	11.2
60 minutes	19.4	18.4	11.5
90 minutes	38	25.6	12.3
120 minutes	49.1	30.1	13
150 minutes	53.3	37.2	13.8
180 minutes	59	42.2	14.7
210 minutes	67.7	47.1	16.2
240 minutes	73.5	52.3	18.4
270 minutes	78	54.7	19.4
300 minutes	83.5	59	19.6
330 minutes	86	62.2	20
360 minutes	91.1	66.3	20.4
390 minutes	93.9	68.1	20.8
420 minutes	96.1	71.3	21.4
450 minutes	98.9	74.5	21.8

Table 3 & 4 the photocatalytic efficiency of the TiO_2 coated Al_2O_3 nanoparticle and Al_2O_3, TiO_2 nanoparticle catalyst was tested by measuring the photocatalyzed discoloration rate of MB in aqueous solution. So the experiment for photodegradation of MB solution under the near UV light source was first set up. Samples of degraded MB solutions taken after different time intervals and their absorbance were measured by the UV- Vis spectrometer to evaluate their concentration change, i.e. degradation rates of MB [18]. The photocatalytic activity of Al_2O_3-TiO_2 particles were evaluated by measuring the decrease of absorbance of MB solution after

addition of Al_2O_3-TiO_2 samples. Table 5 shows the comparative studies of photocatalytic degradation of MB with composite particles calcined at 500 ℃ and uncoated Al_2O_3, TiO_2 at 700 ℃. It was observed that the composite particles calcined at 500 ℃ had higher photocatalytic activity than the other particles calcined at 700 ℃. The higher rate of degradation for the particles thermally treated at 500 ℃ was at tribute to higher crystallinity of titania. Apparently, the degradation of MB by Al_2O_3- TiO_2 was much faster than uncoated Al_2O_3, TiO_2 confirming the important role played by titania as a photocatalyst in the degradation.

XRD analysis
XRD was used to investigate the phase structures and average particle size of the pure TiO_2, Al_2O_3 & Al_2O_3-TiO_2 nanoparticles annealed at 500 ^{o}C. The prepared materials were annealed at 500 ^{o}C before taking the XRD patterns. That characteristics peak of 2θ degree were recognized to the miller indices respectively. Presence of anatase and rutile of TiO_2 is confirmed for both Al_2O_3-TiO_2 nanoparticle. The strongest peak for anatase and rutile were observed at 2θ=25.40 (101) and 2θ=27.50 (110) respectively. The broadening of the peak indicated that the particles were of nanometer scale. The particle size can be estimated from XRD pattern using Scherrer's formula. D=Kλ /cos θ ……(1) where, D is the crystalline size, *K* is a geometrical factor taken to be 0.89, *λ*=1.5406A is the X-ray wavelength, *θ* is the diffraction angle and *β* the peak width at half maximum of the most prominent peaks [19].

Results & Discussion
Scanning Electron Microscopy (SEM) Analysis
The surface morphology of the Al_2O_3, TiO_2 and Al_2O_3-TiO_2 nanoparticles was investigated by SEM measurement. Fig 1 shows the typical SEM images of Al_2O_3, TiO_2 nanoparticles and as prepared Al_2O_3-TiO_2 nanocomposite particles. SEM images show different morphology between Al_2O_3 nanoparticles, TiO_2 nanoparticles and Al_2O_3-TiO_2 nanocomposite particles.
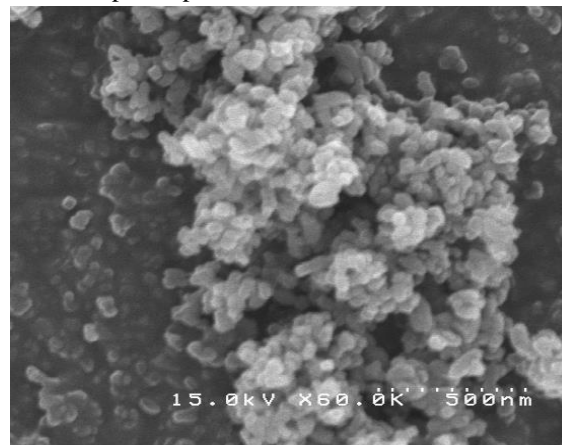
Figure 1: SEM images of Al_2O_3 nanoparticles
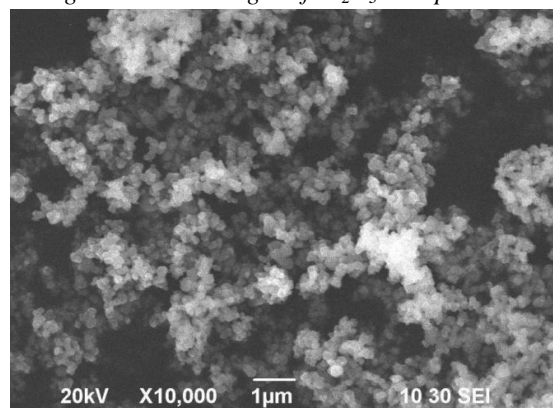
Figure 2: SEM images of TiO_2 nanoparticles
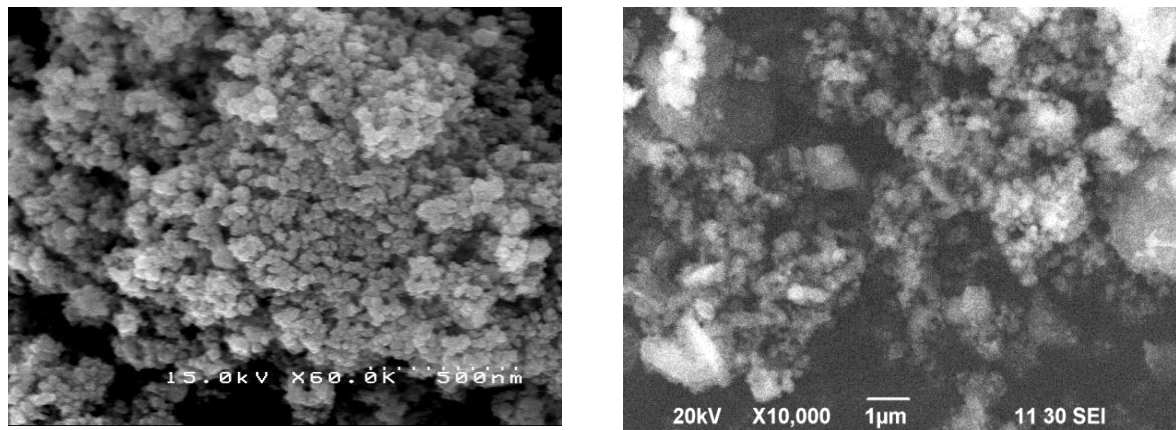
Figure 3: SEM images of Al$_2$O$_3$-TiO$_2$ nanocomposite particles

In figure 1, shows that from Al$_2$O$_3$ particles, which are slightly not uniform to notice, and lot of particles are smaller than 100 nm. From figure 2 shows that, prepared TiO$_2$ particles, which are slightly aggregated to notice, and it is seen that lot of particles are in range between 50-100 nm [20]. From figure 3 shows that, in the composites the Al$_2$O$_3$ and TiO$_2$ particles are well distributed. Whereas the surface morphology had changed after mixing. In composite the brighter particles are Al$_2$O$_3$ and darker are TiO$_2$ due to the higher electron density of Al$_2$O$_3$ to TiO$_2$. The surface of the modified particles is rough and textured, indicating that the Al$_2$O$_3$ particles are dispersed with TiO$_2$ particles in the composite mixture. Al$_2$O$_3$ particles are widely dispersed on in the TiO$_2$ bulks, which would be beneficial to improve the photocatalytic activity.

FT-IR analysis
FT-IR spectrum of Al$_2$O$_3$
Figure 4 shows the FT-IR spectrum of Al$_2$O$_3$ nanoparticles. FTIR spectrum of Al$_2$O$_3$ nanoparticles showed the presence of strong and broad bands at 663cm^{-1} specially showed many bands between 500-750cm^{-1}. It can be seen from figure 18 that the wide absorption peak at 3460cm^{-1} of the surface absorbed water. The band at 520 cm^{-1} indicates Al-O, at 663cm^{-1} indicates Al-O, 3432cm^{-1} and 3672cm^{-1} indicates O-H vibration [21]. The band at 1624cm^{-1} indicates the presence of water on Al$_2$O$_3$ surface.
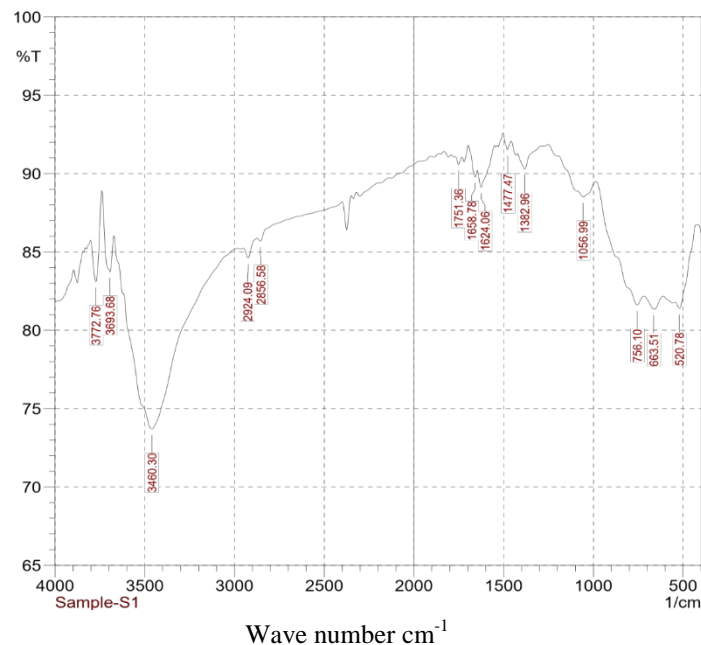
Wave number cm^{-1}
Figure 4: FT IR spectra for Al$_2$O$_3$ nanoparticle

FT-IR spectrum of TiO$_2$

Figure 5 shows the FT-IR spectrum of the samples TiO$_2$. A strong band at 588 cm^{-1} is attributed to Ti-OH stretching vibration. The peak at 1626 cm^{-1} corresponds to the OH bending vibration of the surface of the Ti-OH groups in particles [22]. The broad absorption peak appearing around 3437 cm^{-1} is attributed to the stretching mode of the O-H bond of the surface absorbed water and hydroxyl group, where as the peak at 1400 cm^{-1} is attributed to Ti-O-Ti vibration, present only in sample.
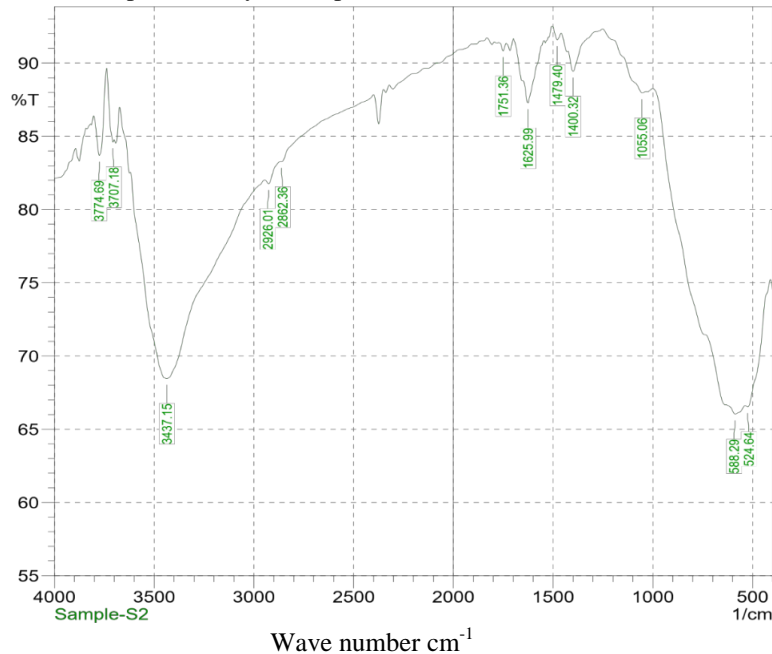
Figure 5: FT IR spectra for TiO$_2$ nanoparticle

FT-IR spectrum of Al$_2$O$_3$-TiO$_2$

Figure 6 shows the FT-IR spectrum of the prepared Al$_2$O$_3$-TiO$_2$ composite particle. The spectrum displayed two characteristics broad band centered at 3441 cm^{-1} and 1614 cm^{-1} which assigned to the stretching and bending modes of vibration of physical adsorbed water on titania surface or to hydroxyl group exists on surface of the oxides respectively. Broad band in the region 450-680cm^{-1} is detected which are associated with the stretching mode of vibrations of bridged Al-O-Al, Ti- O-Ti and Ti-O-Al bonds. The band located at is detected Ti-O-Ti bending mode [23]. So, intensity gradually decrease and that's why crystallinity decreases, therefore amorphous phase shows.
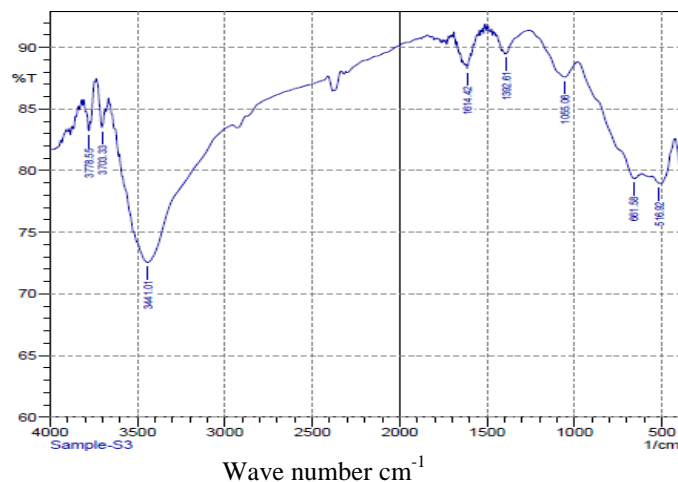
Figure 6: FT IR spectra for Al$_2$O$_3$-TiO$_2$ nanoparticle

XRD spectrum of Al$_2$O$_3$

Figure 7 shows the XRD pattern of Al$_2$O$_3$ nanoparticle were annealed in air at 500°C. Peaks with 2θ values of 18.48, 20.25, 32.1, 36.83, 45.31, 67.04 were observed, which correspond to (100),(002),(101),(102),(104), (112), respectively. No obvious impurity peaks were observed, indicating the high purity of the rutile Al$_2$O$_3$ nanoparticles. These peaks indicate a tetragonal rutile structure of Al$_2$O$_3$ that agree well with documented values for the Al$_2$O$_3$ crystals in the form of powder
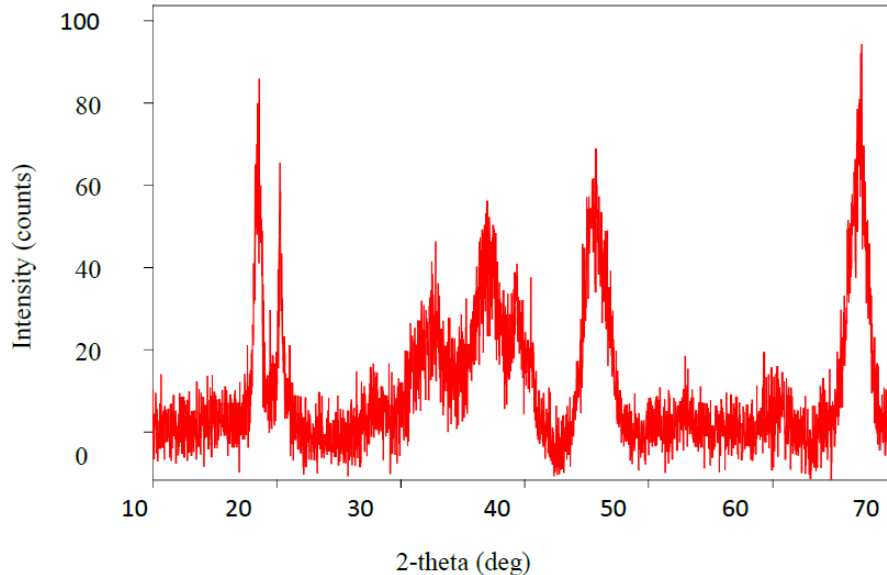
Figure 7: XRD pattern of Al$_2$O$_3$ nanoparticle calcinated at 500 ^{o}C temperature

XRD spectrum of TiO$_2$

Figure 8 shows the XRD pattern of TiO$_2$ nanoparticle calcined at 500 ^{o}C temperature are at 2θ=25.25, 37.77,48.07,53.86,62.68,68.89 positions are corresponding to the planes of (102),(004),(200),(105),(204), (116) respectively of anatase phase of TiO$_2$ .The intense peak observed at 24.2 and 48.3 in fig. are attributed to the anatase phase of TiO$_2$.
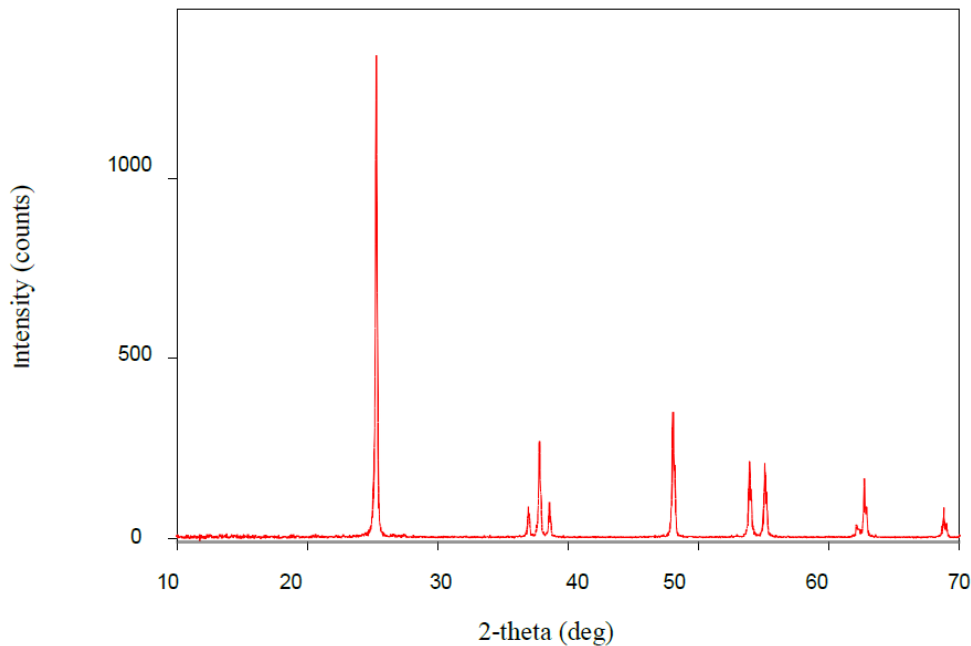
Figure 8: XRD pattern of TiO$_2$ calcinated at 500° C temperature

XRD spectrum of Composites (Al$_2$O$_3$-TiO$_2$)

Figure 9 shows that XRD pattern of Al$_2$O$_3$-TiO$_2$ calcinated at 500 ^{o}C temperature. The 2θ values of 18.48, 20.25, 32.1, 36.83, 45.31, 67.04 were observed, which correspond to (100),(002),(101),(102),(104), (112) respectively and the diffraction peaks at 2θ=25.25, 37.77,48.07,53.86,62.68,68.89 positions are corresponding to the planes of (102),(004),(200),(105),(204), (116) respectively of anatase phase of TiO2. The intense peaks observed at 28.02 and 33.87 in fig. are attributed to the anatase phase of TiO2. No characteristics peaks of AlO and Al are observed in the XRD pattern, indicating that phase-pure Al2O3 can be formed with TiO2 in the Al2O3 -TiO2 composites particles.
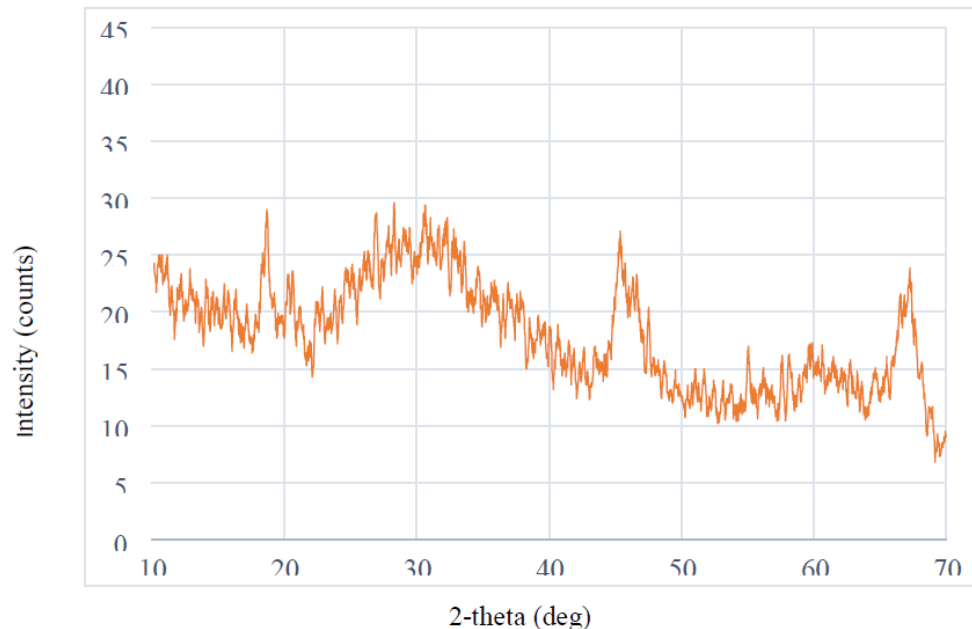
Figure 9: XRD pattern of Al$_2$O$_3$-TiO$_2$ calcinated at 500 ^{o}C temperature

Conclusion

In summary, we have successfully prepared Al$_2$O$_3$-TiO$_2$ nanocomposite particles by ultrasonic method. The coated TiO$_2$ shell on Al$_2$O$_3$ nanoparticle surface was amorphous. Formation of Al-O- Ti bonds between Al$_2$O$_3$ nanoparticle surface and TiO$_2$ layer were confirmed by FT-IR analysis. The spectrum displayed two characteristics broad band centered at 3441 cm^{-1} and 1614 cm^{-1} which assigned to the stretching and bending modes of vibration of physical adsorbed water on titania surface or to hydroxyl group exists on surface of the oxides respectively. So, intensity gradually decrease and that's why crystallinity decreases, therefore amorphous phase shows. The surface characteristic of Al$_2$O$_3$ nanoparticles changed drastically after TiO$_2$ coating as evidenced by SEM. The surface of the modified particles is rough and textured, which would be beneficial to improve photocatalytic activity. From XRD analysis, the intense peak observed at 28.02 and are attributed to the anatase phase of TiO$_2$. Thus XRD pattern, indicating that phase-pure Al$_2$O$_3$ can be formed with TiO$_2$ in the Al$_2$O$_3$-TiO$_2$ composites particles.

Reference

[1]. Dey, S. and Islam, A. (2015) A Review on Textile Waste water Characterization in Bangladesh. *Resources and Environment*, Vol 5(1), pp.15-44

[2]. Pinho, L .and Mosquera, M.J. (2011) Titania-Silica Nano composite Photocatalysts with Application in Stone Self-Cleaning. *The Journal of Physical Chemistry C,* Vol 115, pp. 22851–22862

[3]. Gupta, S.M. and Tripathi, M. (2011) A review of TiO_2 nanoparticles. *Chinese Sci. Bull.*, Vol. 56, No 16, pp. 1639–1657.

[4]. Fu, X. and Qutubuddin, S. (2001) Preparation and Characterization of Titania Nanocoating on Monodisperse Silica Particles. Colloids and Surfaces, Vol 186, pp. 245– 250.

[5]. Suslick, K. S. and Bang, J. H. (2010) Applications of Ultrasound to the Synthesis of Nanostructured Materials. *Advanced Materials*, Vol. 22, pp. 1039–1059 [viewed on 11/06/2013].

[6]. V.P. Kamat, R. Huehn, R. Nicolaescu, A (2002) ''Sense and Shoot''. Approach for photocatalytic degradation of organic contaminants in water, J. Phys. Chem. B 106, 788–794

[7]. H.Y. Lin, Y.Y. Chou, C.L. Cheng, Y.F. Chen, Opt. Express 15 (2007)13832.

[8]. K.S. Suslick, G.J. Price (1999), Applications of ultrasound to materials chemistry, Annu. Rev. Mater. Sci. 29, 295–326.

[9]. Costa, E. D., Zamora, P. P. and Zarbin, A. J. G. (2012) Novel TiO_2/C nanocomposites: Synthesis, characterization, and application as a photocatalyst for the degradation of organic pollutants. *Journal of Colloid and Interface Science*, Vol 368, pp.121–127.

[10]. T.J. Mason, J.P. Lorimer (2002), Applied Sonochemistry. The Uses of Power Ultrasound in Chemistry and Processing, Wiley-VCH Verlag GmbH, Weinheim, Germany.

[11]. L. Nicolais and G. Carotenuto (2005) ''metal-polymer nanocomposites'', Wiley, Hoboken

[12]. M.L. Curridal, R. Comparelli, P.D. Cozzli, G. Mascolo, A. Agostiano (2003), Colloidal oxide nanoparticles for the photocatalytic degradation of organic dye, *Mater. Sci. Eng.*, C (23)285–289

[13]. Shipra Mital.G, ManoiTripathi (2011) ''A review on the synthesis of TiO_2 nanoparticles by solution route'' *Central European Journal of Chemistry* 10(2):279-294

[14]. Radzimska K, Jesionowski T (2014) '' Zinc Oxide from Synthesis to Application: A Review'' *Journal of Material* (7), 2833-2881.

[15]. S.Z. Li, C.L. Gan, H. Cai, C.L. Yuan, J. Guo, P.S. Lee, J. Ma (2007), *Appl. Phys*. Lett.90, 263106

[16]. Ruxangul Jamal; Yakupjan Osman; Adalet Rahman; Ahmat Ali; Yu Zhang and Tursun Abdiryim (2014) ''Solid-State Synthesis and Photocatalytic Activity of Poly terthiophene Derivatives/TiO2 Nanocomposites'' *journal of material* (7), 2833-2881.

[17]. N. Babaei (2006) ''Preparation of TiO_2/Al Nanocomposite Powders via the Ball milling'' First International Congress on Nanoscience and Nanotechnology, Tehran (Iran)

[18]. Nitul Kakati, Seung Hyun Jee, Su Hyun Kim, Jun Young Oh, Young Soo Yoon, (2010) *Thin Solid Films,* (519) 494–498.

[19]. K.V. Baiju, A. Zachariah, S. Shukla, S. Biju, M. L. P. Reddy, K. G. K. Warrier, Catal. Lett. 130 (2009) 130

[20]. R. Vijayalakshmi and V. Rajendran; Arch (2012), *Appl. Sci. Res*., 4 (2):1183-1190

[21]. H. Zhang, X. Quan, S. Chen, H. Zhao (2006), *Enviro. Sci. Technol*. (40) 6104,

[22]. X. T. Wang, S. H. Zhong, X. F. Xiao, J. Mol. Cata. A (2005): *Chem*. 229 (87).

[23]. S. Kalele, R. Dey, N. Hebalkar, J. Urban, S.W. Gosavi and S.K. Kulkarni (2005), *Ind. Academy of Sci*., 65 (5) 787-791.